

The energy-scale-dependent composite operator method for the single-impurity Anderson model

A. Avella^{1,a}, F. Mancini¹, and R. Hayn²

¹ Dipartimento di Fisica “E.R. Caianiello” - Unità di Ricerca INFN di Salerno, Università degli Studi di Salerno, 84081 Baronissi (SA), Italy

² Institut für Festkörper- und Werkstofforschung (IFW) Dresden, 01171 Dresden, Germany

Received 24 September 2003

Published online 9 April 2004 – © EDP Sciences, Società Italiana di Fisica, Springer-Verlag 2004

Abstract. The recently developed energy-scale-dependent Composite Operator Method is applied to the single-impurity Anderson model. A fully self-consistent solution is given and analyzed. At very low temperatures, the density of states presents, on the top of the high-energy background, a Kondo-like peak whose parameter dependence is discussed in detail. The proposed method reproduces the exact results known in the literature with very low numerical effort and it is applicable for arbitrary values of the external parameters.

PACS. 75.50.Ee Antiferromagnetics – 75.30.Et Exchange and superexchange interactions – 75.25.+z Spin arrangements in magnetically ordered materials (including neutron and spin-polarized electron studies, synchrotron-source X-ray scattering, etc.) – 75.50.-y Studies of specific magnetic materials

1 Introduction

The theoretical description of strongly correlated electron systems, like transition-metal oxides [1] and heavy fermion compounds [2], is of high actual interest and effective analytical methods to study them are looked for. A general problem consists in connecting the high- and low-energy scales in a proper way. Methods based on the use of the equations of motion for the Green's functions (e.g., the projection methods [3–13]), usually give a rather reliable description of the high-energy features of strongly correlated systems, but, quite often, the overall solution obtained by their application does not reproduce the low-energy physics accurately enough. Other techniques, like the slave-boson approximation [14], provide a correct picture at low energies but fail at higher ones. However, there is an emerging consensus [15] that in strongly correlated electronic systems we should search for a correct description of both energy scales at once. The anomalous behaviors shown by these systems are caused and/or influenced by both the broad incoherent spectral features far away from the Fermi level and the more dispersive quasi-particle bands close to it. Recently [16], it was shown how the Composite Operator Method [12,13] (COM) could be used to resolve coherent low-energy features in a proper way by solving the SU(N) Kondo model.

The Kondo model should be considered just as a first step. It contains no charge degrees of freedom of the strongly correlated impurity level, and it is usually not

sufficient for a realistic description of $4f$ -electron spectra. For this latter purpose the single-impurity Anderson model is much better suited [2]. Furthermore, the solution of the Anderson model is a building block within the Dynamical Mean Field Theory [15] (DMFT) algorithm, which has favored large progresses in the comprehension of the Mott metal-insulator transition phenomenon. The single-impurity Anderson model is well and widely studied [17], but the reliable methods are rather involved (e.g., quantum Monte Carlo method [18], Bethe ansatz [19], numerical renormalization group [20] and non-crossing approximation [17]) and require a quite huge computational effort. This is certainly an obstacle to use them within the DMFT algorithm or to interpret the realistic spectra of rare-earth compounds. According to this, we present here a simple analytical method to solve the single-impurity Anderson model, which is capable to reproduce both the high- and the low-energy features, as known after the exact solution [17], in a reasonable way and, practically, without requiring any computational effort at all.

2 Hamiltonian and equations of motion

The single-impurity Anderson model is defined by the Hamiltonian

$$H = \sum_{\mathbf{k},\sigma} \varepsilon_{\mathbf{k}} c_{\mathbf{k}\sigma}^\dagger c_{\mathbf{k}\sigma} + \sum_{\sigma} \varepsilon_f f_{\sigma}^\dagger f_{\sigma} + U n_{f\downarrow} n_{f\uparrow} + \frac{V}{\sqrt{N}} \sum_{\mathbf{k},\sigma} \left(c_{\mathbf{k}\sigma}^\dagger f_{\sigma} + f_{\sigma}^\dagger c_{\mathbf{k}\sigma} \right), \quad (2.1)$$

^a e-mail: avella@sa.infn.it

where $c_{\mathbf{k}\sigma}$ represents the electrons in the valence band ($\varepsilon_{\mathbf{k}}$) and f_{σ} those at the impurity level (ε_f); $n_{f\sigma}$ is the density charge operator for the f -electrons of spin σ , N is the number of sites, U is the Coulomb repulsion at the impurity level and V is the strength of the hybridization between the valence band and the impurity level. For the sake of simplicity, we restrict ourselves to a simple two (spin) degenerate impurity level ($\sigma = \pm 1$, $\bar{\sigma} = -\sigma$).

The first step within any method based on the projection technique consists in individuating an appropriate set of basis operators. In fact, for strongly correlated systems the original electronic operators are just the wrong place where to start any approximate treatment [21]. The electrons completely lose their identities owing to the strong interactions and other complex excitations appear. These latter are the only effective quasi-particles present in the systems and only in terms of them any description of the dynamics should be attempted. The basis (composite) operators should be then chosen in order to describe such excitations. The choice is not easy, but some recipes could be given [22]. In the present case one should have as minimal requirement an appropriate description of the free propagation of c -electrons and the atomic dynamics of f -electrons. The latter have two possible excitations corresponding to the transitions from $|0\rangle_f$ to $|\sigma\rangle_f$ and from $|\sigma\rangle_f$ to $|\uparrow\downarrow\rangle_f$. That leads to the first three basis operators

$$\begin{aligned}\psi_{1\sigma} &= c_{0\sigma} = \frac{1}{\sqrt{N}} \sum_{\mathbf{k}} c_{\mathbf{k}\sigma} \\ \psi_{2\sigma} &= \xi_{\sigma} = (1 - n_{f\bar{\sigma}}) f_{\sigma} \\ \psi_{3\sigma} &= \eta_{\sigma} = n_{f\bar{\sigma}} f_{\sigma}.\end{aligned}\quad (2.2)$$

It is worth noting that $\psi_{2\sigma} = \xi_{\sigma} = X^{0\sigma}$ and $\psi_{3\sigma} = \eta_{\sigma} = \sigma X^{\bar{\sigma}2}$ are the Hubbard operators describing the lower- and the upper-Hubbard subbands.

These three operators give a very good description of the high-energy features, but are certainly insufficient to describe the low-energy ones and the mixing between the two regimes. Then, in order to overcome such limitations, we write down the equations of motion for the operators (2.2)

$$\begin{aligned}i\partial_t c_{\mathbf{k}\sigma} &= [c_{\mathbf{k}\sigma}, H] = \varepsilon_{\mathbf{k}} c_{\mathbf{k}\sigma} + \frac{V}{\sqrt{N}} (\xi_{\sigma} + \eta_{\sigma}) \\ i\partial_t \xi_{\sigma} &= [\xi_{\sigma}, H] = \varepsilon_f \xi_{\sigma} + \frac{V}{2} c_{0\sigma} + V \pi_{\sigma} \\ i\partial_t \eta_{\sigma} &= [\eta_{\sigma}, H] = (\varepsilon_f + U) \eta_{\sigma} + \frac{V}{2} c_{0\sigma} - V \pi_{\sigma},\end{aligned}\quad (2.3)$$

and account for the appearance of a new operator, namely the fluctuation field

$$\pi_{\sigma} = \psi_{4\sigma} + \psi_{5\sigma} + \psi_{6\sigma},\quad (2.4)$$

with

$$\begin{aligned}\psi_{4\sigma} &= \frac{1}{2} (1 - n_f) c_{0\sigma} \\ \psi_{5\sigma} &= \sigma c_{0\sigma} S^z + c_{0\bar{\sigma}} S^{\bar{\sigma}} \\ \psi_{6\sigma} &= c_{0\bar{\sigma}}^{\dagger} f_{\bar{\sigma}} f_{\sigma},\end{aligned}\quad (2.5)$$

where $n_f = n_{f\uparrow} + n_{f\downarrow}$, $S^z = (n_{f\uparrow} - n_{f\downarrow})/2$ and $S^{\sigma} = f_{\sigma}^{\dagger} f_{\bar{\sigma}}$. The fluctuation field π describes the coupling of the valence band to density-, spin- and pair-impurity fluctuations and opens the possibility to study the low-energy dynamics connected with them. According to this, we have decided to include also the operators (2.5) into the basis and study the system in terms of this set of six basic excitations. Such basis cannot be considered complete according to the fact that an infinite degree of freedom system possesses an infinite number of operator basis. Then, it is obvious that the basis is neither unique. In particular, it has been already mentioned above that many recipes can be used in order to construct an operatorial basis, each according to the features of interest. However, as we will see from the obtained results, this basis seems sufficient to catch the main features of the dynamics of this system.

In order to be more compact, we rewrite the six basis operators in spinorial notation

$$\begin{aligned}\psi_1 &= c_0 = \frac{1}{\sqrt{N}} \sum_{\mathbf{k}} c_{\mathbf{k}} & \psi_4 &= \frac{1}{2} (1 - n_f) c_0 \\ \psi_2 &= \xi = (1 - n_f) f & \psi_5 &= \frac{1}{2} \vec{\sigma} \circ \vec{n}_f \cdot c_0 \\ \psi_3 &= \eta = n_f f & \psi_6 &= c_0^{\dagger} \cdot \xi \otimes \eta.\end{aligned}\quad (2.6)$$

Here $\vec{n}_f = f^{\dagger} \cdot \vec{\sigma} \cdot f$, $\vec{\sigma}$ are the Pauli matrices, \cdot denotes the scalar product in spin space, \circ the scalar product in direct space and \otimes the tensor product. This notation will be used hereafter. It should be noted that the exact expressions of the basis operators have been chosen such that they transform under the particle-hole transformation ($c_0 \rightarrow c_0^{\dagger}$ and $f \rightarrow f^{\dagger}$) into themselves or into another basis operator: $\psi_1 \rightarrow \psi_1^{\dagger}$, $\psi_2 \rightarrow \psi_3^{\dagger}$, $\psi_3 \rightarrow \psi_2^{\dagger}$ and $\psi_n \rightarrow -\psi_n^{\dagger}$ for $n = 4, 5, 6$.

As next step, we derive the equations of motion for the retarded Green's functions (GF)

$$\begin{aligned}G_{nm}(\omega) &= \mathcal{F} \langle \mathcal{R} [\psi_n(t) \psi_m^{\dagger}(t')] \rangle \\ &= \mathcal{F} [\theta(t - t') \langle \{ \psi_n(t), \psi_m^{\dagger}(t') \} \rangle]\end{aligned}\quad (2.7)$$

where \mathcal{F} stays for the Fourier transform and \mathcal{R} for the retarded time ordering operator. The inhomogeneous term in the equations of motion for the Green's functions G_{nm} is constituted by the normalization matrix (its expression in terms of basic field correlators is given in Eq. (A.1) of Appendix A)

$$I_{nm} = \langle \{ \psi_n(t), \psi_m^{\dagger}(t) \} \rangle,\quad (2.8)$$

where $\{-, -\}$ stays for the anticommutator and $\langle - \rangle$ for the thermal average. The normalization matrix is not only fundamental to derive the Green's functions but provides also important information about the total spectral weights of the fields. Its matrix elements depend on the expectation values $C_{ij} = \langle \psi_i \psi_j^{\dagger} \rangle$ (correlation matrix). It contains for instance the average charge density at the impurity level $\langle n_f \rangle = 2(1 - C_{22} - C_{33})$, and the double occupancy $D_f = \langle n_{f\uparrow} n_{f\downarrow} \rangle = 1 - C_{22} - 2C_{33}$. For further use we define also the matrix elements with the fluctuation

field, i.e., $I_{n\pi} = \langle \{\psi_n(t), \pi^\dagger(t)\} \rangle$. Then, after the equations of motion (2.3), we have the following expressions for the Green's functions

$$\begin{aligned} G_{11} &= \Gamma_0 + V^2 \Gamma_0^2 (G_{22} + 2G_{23} + G_{33}) \\ G_{22} &= I_{22} \frac{\Gamma_+}{F} + \frac{B_+^2}{F^2} G_{\pi\pi} + \frac{B_+(C_+ + x_+ C_-)}{F^2} \\ G_{33} &= I_{33} \frac{\Gamma_-}{F} + \frac{B_-^2}{F^2} G_{\pi\pi} - \frac{B_-(C_- + x_- C_+)}{F^2} \\ G_{23} &= x_- G_{22} - \frac{V\Gamma_-}{F} (B_+ G_{\pi\pi} + C_+ + x_+ C_-) \end{aligned} \quad (2.9)$$

where we introduced the following abbreviations

$$\begin{aligned} \Gamma_0 &= \frac{1}{N} \sum_{\mathbf{k}} \frac{1}{\omega - \varepsilon_{\mathbf{k}}} & \Gamma_s &= \frac{1}{\omega - \varepsilon_s - V^2 \Gamma_0 / 2} \\ x_s &= \frac{1}{2} V^2 \Gamma_0 \Gamma_s & B_s &= V \Gamma_s - V x_s \Gamma_{\bar{s}} \\ C_+ &= \left(I_{2\pi} + \frac{1}{2} V \Gamma_0 I_{1\pi} \right) \Gamma_+ & C_- &= \left(I_{3\pi} + \frac{1}{2} V \Gamma_0 I_{1\pi} \right) \Gamma_- \\ F &= 1 - x_+ x_- \end{aligned} \quad (2.10)$$

with $s = \pm$, $\bar{s} = -s$, $\varepsilon_+ = \varepsilon_f$, and $\varepsilon_- = \varepsilon_f + U$, to shorten the notation. It is worth noticing that $\Gamma_0(\omega)$ is just the free ($V = 0$) propagator for c_0 operator. We see from (2.9) that we can calculate the Green's function for the valence electrons G_{11} and the f -impurity $G_{ff} = G_{22} + 2G_{23} + G_{33}$ once we know the Green's function of the fluctuation field $G_{\pi\pi}$.

3 High- and low-energy scales

In order to resolve the low-energy features embedded in the high-energy background, following the idea given in reference [16], which is based on the well-established physical assumption that at low energies we have a quasi-particle theory [17] as also derived by the slave-boson theory [14], we split the dynamics of the fluctuation field into an high- and a low-energy part. As the essence of the Kondo effect consists in the coupling of the valence band to the spin fluctuations at the impurity level, we split only ψ_5 as

$$\psi_5 = \psi_5^H + \psi_5^L \quad (3.1)$$

and assume instead that the charge (ψ_4) and the pair (ψ_6) terms in the fluctuation field are sufficiently well represented by their high-energy parts only ($\psi_4 = \psi_4^H$ and $\psi_6 = \psi_6^H$). In practice, we assume that the low-energy field ψ_5^L spans a different energy sector of the Hilbert space with respect to ψ_5^H , ψ_4 , ψ_6 , and describes a coherent quasi-particle at very low energies; energies that are much smaller than any other defined in the Hamiltonian. According to this, we make the following ansatz

$$i\partial_t \psi_5^L = [\psi_5^L, H] = \kappa_1 c_0 + \kappa_2 \xi + \kappa_3 \eta. \quad (3.2)$$

The coefficients κ_i ($i = 1, 2, 3$) are determined by projecting onto the basis (2.6)

$$\begin{aligned} \kappa_1 &= V (I_{25}^L + I_{35}^L) \\ \kappa_2 &= \varepsilon_f I_{25}^L / I_{22} + V I_{55}^L / (2I_{22}) \\ \kappa_3 &= (\varepsilon_f + U) I_{35}^L / I_{33} - V I_{55}^L / (2I_{33}) \end{aligned} \quad (3.3)$$

with

$$I_{5i}^L = \left\langle \left\{ \psi_5^L, \psi_i^\dagger \right\} \right\rangle. \quad (3.4)$$

After equation (3.1) and the above reported consequent reasoning, we split the still unknown Green's function $G_{\pi\pi} = \mathcal{F}\langle \mathcal{R} [\pi(t)\pi(t')] \rangle$ into a low-energy component $G_{\pi\pi}^L = \mathcal{F}\langle \mathcal{R} [\pi^L(t)\pi^L(t')] \rangle = \mathcal{F}\langle \mathcal{R} [\psi_5^L(t)\psi_5^L(t')] \rangle = G_{55}^L$ and in a high-energy one $G_{\pi\pi}^H = \mathcal{F}\langle \mathcal{R} [\pi^H(t)\pi^H(t')] \rangle = \sum_{n,m=4}^6 \mathcal{F}\langle \mathcal{R} [\psi_n^H(t)\psi_m^H(t')] \rangle$. We neglect the cross-term $\mathcal{F}\langle \mathcal{R} [\pi^L(t)\pi^H(t')] \rangle$ according to our previous assumption of no-overlap of the energy sectors spanned by ψ_5^L and all other fields involved. According to equation (3.2), G_{55}^L obeys the following equation of motion

$$\omega G_{55}^L = I_{55}^L + \kappa_1 G_{15}^L + \kappa_2 G_{25}^L + \kappa_3 G_{35}^L \quad (3.5)$$

where $G_{i5}^L = \mathcal{F}\langle \mathcal{R} [\psi_i(t)\psi_5^L(t')] \rangle$. Then, for the sake of consistency, we approximate G_{i5}^L (see Appendix B for complete expressions) only by those components that are explicitly proportional to G_{55}^L , i.e.,

$$\begin{aligned} G_{15}^L &= V \Gamma_0 (G_{25}^L + G_{35}^L) \\ G_{25}^L &= \frac{B_+}{F} G_{55}^L \\ G_{35}^L &= -\frac{B_-}{F} G_{55}^L \end{aligned} \quad (3.6)$$

and we finally obtain

$$\begin{aligned} G_{\pi\pi}^L &= G_{55}^L = \frac{I_{55}^L}{\omega - \Omega_0} \\ \Omega_0 &= \frac{(\kappa_1 V \Gamma_0 + \kappa_2) B_+ - (\kappa_1 V \Gamma_0 + \kappa_3) B_-}{2F}. \end{aligned} \quad (3.7)$$

It is worth noticing that, in determining the actual expressions for G_{i5}^L , we have neglected both the cross-terms $\mathcal{F}\langle \mathcal{R} [\psi_i^H(t)\psi_5^L(t')] \rangle$ with $i = 4, 5, 6$, according to our previous assumption of no-overlap of the energy sectors, and those terms proportional to Γ and Γ_s , according to the well-defined high-energy character of these latter.

We are now left with the task of computing the high-energy contribution $G_{\pi\pi}^H = \sum_{n,m=4}^6 G_{nm}^H$ where $G_{nm}^H = \mathcal{F}\langle \mathcal{R} [\psi_n^H(t)\psi_m^H(t')] \rangle$. In order to accomplish this task, we use the mode-coupling approximation [23], also known as self-consistent Born approximation. In practice, we neglect the mixing terms among different bosonic modes (i.e., we take $G_{45}^H = G_{46}^H = G_{56}^H = 0$) and decouple the remaining corresponding time-ordered propagators in terms of the charge ($S_0 = \mathcal{F}\langle \mathcal{T} [n_f(t)n_f(t')] \rangle$), spin ($S_z = \mathcal{F}\langle \mathcal{T} [S^z(t)S^z(t')] \rangle$) and

pair ($S_p = \mathcal{F}\langle T [f_{\downarrow}(t)f_{\uparrow}(t)f_{\uparrow}^{\dagger}(t')f_{\downarrow}^{\dagger}(t')] \rangle$) impurity time-ordered propagators, and of the valence electron time-ordered propagator (S_{11}). For instance, we have

$$S_{55}^H(\omega) = 3 \frac{i}{2\pi} \int d\Omega S_z(\omega - \Omega) S_{11}(\Omega). \quad (3.8)$$

Actually, for energies as high as those we intend to describe in the high-energy sector and as far as the impurity level is not too deep inside the valence band (i.e., for $|\varepsilon_f|$ not too small with respect to the bandwidth) we can safely take the atomic limit for the spin, charge and pair impurity propagators. In the high-energy regime, any other treatment would not substantially affect our results (i.e., by taking the atomic limit we already get an accuracy of the same order of the energy scale we are computing). For instance, we have

$$S_z(\omega) = -\frac{1}{4} 2i\pi [\langle n_f \rangle - 2D_f] \delta(\omega). \quad (3.9)$$

Then, in the symmetric case ($-2\varepsilon_f = U$, leading to $\langle n_f \rangle = 1$), all the non-zero contributions are proportional to G_{11} , namely

$$\begin{aligned} G_{44}^H &= \frac{1}{4}(1 - \langle n_f \rangle + 2D_f)G_{11} \\ G_{55}^H &= \frac{3}{2}(\langle n_f \rangle/2 - D_f)G_{11} \\ G_{66}^H &= -D_f G_{11}. \end{aligned} \quad (3.10)$$

Finally, we can write the following expression for the fluctuation field Green's function $G_{\pi\pi}$, which take into account both high- and low-energy contributions

$$G_{\pi\pi} = \left(\frac{1}{4} + \frac{\langle n_f \rangle}{2} - 2D_f \right) G_{11} + G_{55}^L. \quad (3.11)$$

For ε_f outside the valence band we have numerically checked that the influence of the double occupancy D_f in equation (3.11) is very small and could be neglected. This latter procedure has been adopted in the asymmetric case (as U has always been taken much larger than the bandwidth) with the result that equation (3.11), with $D_f = 0$, also holds.

It is worth noting that the high-energy Green's function G_{55}^H exhausts only part of the spectral weight I_{55} , as expected from an independent evaluation of normalization matrix,

$$\lim_{\omega \gg 1} G_{55}^H = \frac{3}{4} \frac{(\langle n_f \rangle - 2D_f)}{\omega} \neq \frac{I_{55}}{\omega} = \lim_{\omega \gg 1} G_{55} \quad (3.12)$$

which can be derived from (3.10) using $\lim_{\omega \gg 1} G_{11} = 1/\omega$. On the contrary, we have: $\lim_{\omega \gg 1} \omega G_{44}^H = I_{44} = \lim_{\omega \gg 1} G_{44}$ and $\lim_{\omega \gg 1} \omega G_{66}^H = I_{66} = \lim_{\omega \gg 1} G_{66}$. This consideration is fundamental as explains why we are allowed/forced to consider the possibility of a low-energy contribution to the dynamics and why we can/have to concentrate on the spin fluctuations.

4 Self-consistency

In order to finally compute the GF in a self-consistent way, one has to take into account two aspects. First of all, we have to determine the matrix elements of the normalization matrix by calculating the expectation values

$$C_{ij} = \langle \psi_i \psi_j^{\dagger} \rangle = \int d\omega [1 - f_F(\omega)] A_{ij}(\omega) \quad (4.1)$$

where $A_{ij}(\omega) = -\frac{1}{\pi} \Im[G_{ij}(\omega)]$ and f_F is the Fermi function. Second, a self-consistent calculation of the low-energy parts of the spectral weights I_{25}^L , I_{35}^L , and I_{55}^L is needed in order to determine G_{55}^L (see Eq. (3.6)). For that purpose we start from the total spectral weights $I_{25} = -3C_{12}/2$, $I_{35} = -3C_{13}/2$, and $I_{55} = \frac{3}{4}(\langle n_f \rangle - 2D_f) + C_{15}$. Then, for a given temperature T and for given low-energy contributions I^L , one can determine the total weights I , written schematically as $I[T, I^L]$, by exploiting the well-known connection between the correlation and the Green's function matrices (4.1). To extract the weight connected with the low-energy part, we compare the spectral weights calculated for $I^L = 0$ (defining $I^H[T] = I[T, I^L = 0]$) with the complete expression. Then, the required self-consistency condition can be written as

$$I^L[T] = I[T, I^L] - I^H[T]. \quad (4.2)$$

This procedure has demonstrated to be capable to grasp part of the effects connected with the mixing between the high- and low-energy sectors. To calculate C_{12} , C_{13} , and C_{15} we need also the corresponding Green's functions whose expressions are given in the Appendix B for completeness.

5 Numerical results

The numerical calculations have been performed with a density of states for the valence band electrons $c_{\mathbf{k}\sigma}$ which is constant and finite only between energies $-D$ and D . That is, we have used a free ($V = 0$) propagator $\Gamma_0(\omega)$ for c_0 with the following well-known expression [24]

$$\Gamma_0(\omega) = \frac{1}{2D} \ln \left| \frac{D + \mu + \omega}{D - \mu - \omega} \right| - \frac{i\pi}{2D} \theta(D - |\omega + \mu|). \quad (5.1)$$

We have given the formula for an arbitrary value of the chemical potential μ . The expectation values at finite temperature T have been calculated by means of the Matsubara formalism

$$C_{lm} = -2T \Re \left[\sum_{n=0}^{\infty} \left(G_{lm}(i\omega_n) - \frac{I_{lm}}{i\omega_n - \varepsilon} \right) \right] + [1 - f_F(\varepsilon)] I_{lm} \quad (5.2)$$

where $\omega_n = (2n + 1)\pi T$. The arbitrary small number $0 < \varepsilon \ll 1$ and the Fermi function f_F have been introduced in order to ensure the correct behavior at high frequencies.

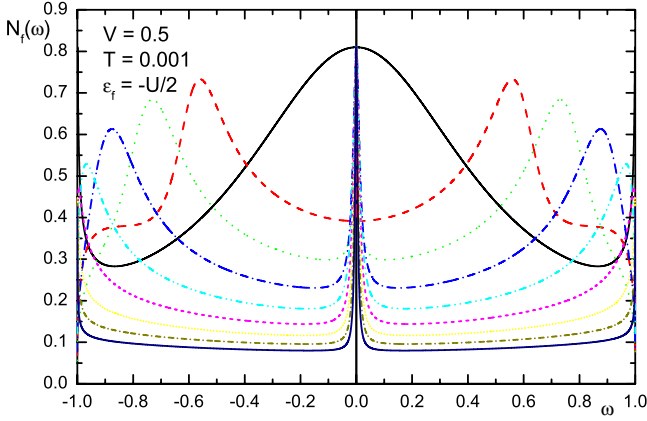


Fig. 1. Impurity density of states in the symmetric case for different positions of the impurity level. The parameters are $V = 0.5$, $T = 0.001$, $D = 1$, and $U = 0, 1.2, 1.6, 2.0, \dots, 4$.

The zero-order Green's function along the imaginary axis is given by

$$G_0(i\omega) = \frac{1}{2D} \ln \sqrt{\frac{(D + \mu)^2 + \omega^2}{(D - \mu)^2 + \omega^2}} + \frac{i}{2D} \left(\arctan \frac{\omega}{D + \mu} + \arctan \frac{\omega}{D - \mu} - \pi \right). \quad (5.3)$$

Let us start the discussion regarding our results with a short briefing about the high-energy features. It is worth noticing that our solution manage to describe the physics at the energy scale of U in a very effective way by explicitly taking into account the excitations related to the Hubbard subbands. In Figure 1, in fact, we can clearly see that the relevant features are correctly reproduced: the splitting of the non-interacting band into two subbands for finite values of U , a distance in energy between the centers of mass of the two subbands almost equal to U , spectral weights independent of bare U , but strongly dependent on the ratio V/U . As regards the scale of energy V , we use a basis rich enough to give the exact solution in absence of U : second order (V^2) resonant behavior, spectral weights satisfying the ordinary sum rules. Then, higher order processes ruled by the competition of these two scales of energy (the localizing U and the dispersing V), and strictly dependent only on the ratio V/U , are just those responsible for the low-energy features we will discuss in the following paragraphs.

We can now move to the study of the low-energy features (whose description is the actual goal of this manuscript) and, in particular, to the analysis of the evolution of the Kondo peak by moving the impurity level towards the valence band in the symmetric case (see Fig. 1). The peak is widened for decreasing values of $|\varepsilon_f|$ outside of the band. In that case we have two bound-states at roughly $\pm\varepsilon_f$ which are not shown in Figure 1. For $|\varepsilon_f|$ inside of the band we can observe a characteristic three peak structure. Remarkably, the central peak height is not changed and identical to the height for $U = 0$, in agreement with the Friedel sum rule. All these features are in

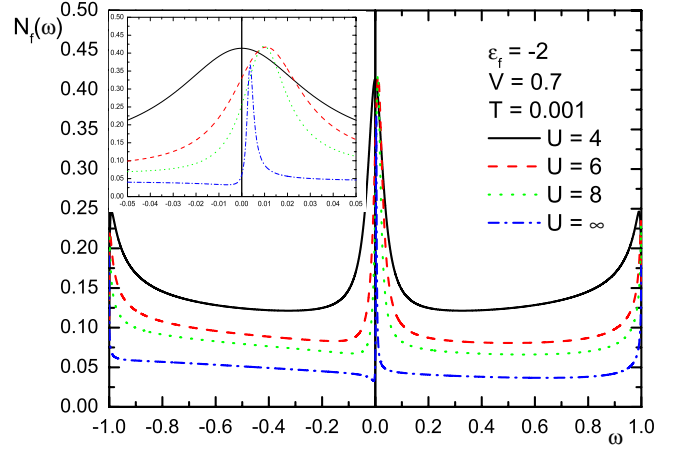


Fig. 2. Kondo peak in the asymmetric case with the parameters $\varepsilon_f = -2$, $V = 0.7$, $D = 1$, $\mu = 0$, and $T = 0.001$. The width of the Kondo peak diminishes with increasing Hubbard correlation U [$I_{55}^L = 0.374$ for $U = 4$ (symmetric case), 0.287 for $U = 6$, 0.215 for $U = 8$ and 0.068 for $U = \infty$].

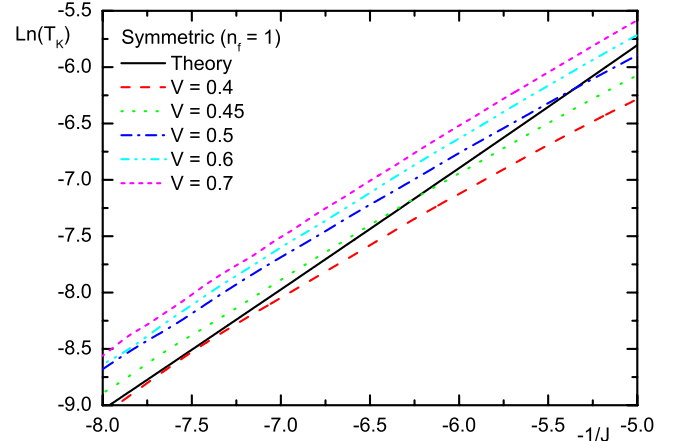


Fig. 3. Kondo-temperature in the symmetric case in dependence on the exchange coupling J compared with the formula given in the text.

agreement with the exact behavior known from the numerical renormalization group [17].

Figure 2 shows results in the asymmetric case. The Kondo peak is shifted slightly above the Fermi level and its shape becomes asymmetric. Furthermore, the width of the Kondo peak is decreased in agreement with the reduction of the Kondo temperature. It is worth noting that the Kondo peak also remains for $U \rightarrow \infty$. If we increase the temperature, the Kondo peak vanishes by diminishing its width (not shown). We have defined the Kondo temperature as the one at which the parameter I_{55}^L has a change in the concavity when plotted as a function of the temperature. The Kondo temperature becomes exponentially small for small values of $J = V^2(1/|\varepsilon_f| + 1/|\varepsilon_f + U|)$ in agreement (see Fig. 3) with the formula [17] $T_K = D\sqrt{2J\rho_0} \exp[-1/(2J\rho_0)]$, where $\rho_0 = 1/(2D)$ is the density of states of the unperturbed valence band at the Fermi level. It is worth noting that this formula is correct only in

$$I = \begin{pmatrix} 1 & 0 & 0 & \frac{1}{2}(1 - \langle n_f \rangle) & 0 & 0 \\ 0 & 1 - \langle n_f \rangle / 2 & 0 & -\frac{1}{2}C_{12} & -\frac{3}{2}C_{12} & C_{13} \\ 0 & 0 & \langle n_f \rangle / 2 & -\frac{1}{2}C_{13} & -\frac{3}{2}C_{13} & C_{12} \\ \frac{1}{2}(1 - \langle n_f \rangle) & -\frac{1}{2}C_{12} & -\frac{1}{2}C_{13} & \frac{1}{4}(1 - \langle n_f \rangle) + \frac{1}{2}D_f & 0 & \frac{1}{2}C_{16} \\ 0 & -\frac{3}{2}C_{12} & -\frac{3}{2}C_{13} & 0 & \frac{3}{4}(\langle n_f \rangle - 2D_f) + C_{15} & 0 \\ 0 & C_{13} & C_{12} & \frac{1}{2}C_{16} & 0 & D_f + C_{14} \end{pmatrix} \quad (\text{A.1})$$

the symmetric case and for $J \ll D$. We have a strong dependence on the value of the hybridization V that shows a lack of universality. Anyway, the linear behavior at small J is preserved for any value of V showing that the exponential dependence, which is not possible to obtain perturbatively, is correctly described. We also studied the infinite bandwidth case, but it does not give any qualitative change to the physical picture described above.

In conclusion, a recently developed energy-scale-dependent approach [16], which is capable to reproduce in a reasonable way both high- and low-energy features of known exact solutions of impurity models, has been extended to the case where relevant charge fluctuations are present. The originating procedure, the Composite Operator Method [12, 13], provides a fully self-consistent solution where, on the top of a broad high-energy background, a Kondo peak is present at low temperatures. The parameter dependencies of the peak features and of the Kondo temperature have been correctly reproduced, with respect to the exact results known in the literature, with very low numerical effort.

A.A. wishes to thank Dario Villani and Gabriel Kotliar for many useful discussions on the subject and for all the preliminary work done together.

Appendix A: The normalization matrix

The normalization matrix is found to be

see equation (A.1) above.

Appendix B: The self-consistency cycle

To close the self-consistency cycle, the following GF are needed

$$G_{12} = VI_0(G_{22} + G_{23}) \quad G_{13} = VI_0(G_{23} + G_{33}), \quad (\text{B.1})$$

and

$$\begin{aligned} G_{15} &= VI_0(G_{25} + G_{35}) \\ G_{25} &= \frac{B_+}{F}G_{\pi 5} + \frac{(C_{5+} + x_+C_{5-})}{F} \\ G_{35} &= -\frac{B_-}{F}G_{\pi 5} + \frac{(C_{5-} + x_-C_{5+})}{F} \end{aligned} \quad (\text{B.2})$$

where we have in close analogy to (3.11)

$$G_{\pi 5} = \frac{3}{2} \left(\frac{\langle n_f \rangle}{2} - D_f \right) G_{11} + G_{55}^L \quad (\text{B.3})$$

and $C_{5+} = I_{25}\Gamma_+$, and $C_{5-} = I_{35}\Gamma_-$.

References

1. M. Imada, A. Fujimori, Y. Tokura, *Rev. Mod. Phys.* **70**, 1039 (1998)
2. O. Gunnarsson, K. Schönhammer, *Many-Body Formulation of Spectra of Mixed Valence Systems* (Elsevier Science, 1987), Vol. 10, p. 103
3. H. Mori, *Progr. Theor. Phys.* **33**, 423 (1965); H. Mori, *Progr. Theor. Phys.* **34**, 399 (1965)
4. D.J. Rowe, *Rev. Mod. Phys.* **40**, 153 (1968)
5. L.M. Roth, *Phys. Rev.* **184**, 451 (1969)
6. W. Nolting, *Z. Phys.* **255**, 25 (1972)
7. Y.A. Tserkovnikov, *Teor. Mat. Fiz.* **49**, 219 (1981)
8. W. Nolting, W. Borgiel, *Phys. Rev. B* **39**, 6962 (1989)
9. N.M. Plakida, V.Y. Yushankhai, I.V. Stasyuk, *Physica C* **162–164**, 787 (1989)
10. A.J. Fedro, Y. Zhou, T.C. Leung, B.N. Harmon, S.K. Sinha, *Phys. Rev. B* **46**, 14785 (1992)
11. P. Fulde, *Electron Correlations in Molecules and Solids*, 3rd edn. (Springer-Verlag, 1995)
12. F. Mancini, S. Marra, H. Matsumoto, *Physica C* **244**, 49 (1995); F. Mancini, S. Marra, H. Matsumoto, *Physica C* **250**, 184 (1995); F. Mancini, S. Marra, H. Matsumoto, *Physica C* **252**, 361 (1995); A. Avella, F. Mancini, R. Münzner, *Phys. Rev. B* **63**, 245117 (2001); V. Fiorentino, F. Mancini, E. Zanas, A.F. Barabanov, *Phys. Rev. B* **64**, 214515 (2001)
13. S. Ishihara, H. Matsumoto, S. Odashima, M. Tachiki, F. Mancini, *Phys. Rev. B* **49**, 1350 (1994); H. Matsumoto, T. Saikawa, F. Mancini, *Phys. Rev. B* **54**, 14445 (1996); H. Matsumoto, F. Mancini, *Phys. Rev. B* **55**, 2095 (1997)

14. S.E. Barnes, *J. Phys. F* **6**, 1375 (1976)
15. A. Georges, G. Kotliar, W. Krauth, M.J. Rozenberg, *Rev. Mod. Phys.* **68**, 13 (1996)
16. D. Villani, E. Lange, A. Avella, G. Kotliar, *Phys. Rev. Lett.* **85**, 804 (2000)
17. A.C. Hewson, *The Kondo Problem to Heavy Fermions* (Cambridg University Press, Cambridge, 1997)
18. J. Hirsch, R. Fye, *Phys. Rev. Lett.* **56**, 2521 (1986)
19. P. Wiegmann, A. Tselick, *J. Phys. C.* **12**, 2281, 2321 (1983)
20. K. Wilson, *Rev. Mod. Phys.* **47**, 773 (1975)
21. F. Mancini, A. Avella, *Eur. Phys. J. B* **36**, 37 (2003)
22. We can choose: the higher order fields emerging from the equations of motion (i.e., the conservation of some spectral moments is assured) [25], the eigenoperators of some relevant interacting terms (i.e., the relevant interactions are correctly treated) [26], the eigenoperators of the problem reduced to a small cluster [27], the composite field describing the Kondo-like singlet emerging at low-energy in any electronic spin system [16], ...
23. J. Bosse, W. Götze, M. Lücke, *Phys. Rev. A* **17**, 434 (1978)
24. G. Mahan, *Many-Particle Physics* (Plenum Press, New York, 1990)
25. F. Mancini, *Phys. Lett. A* **249**, 231 (1998)
26. A. Avella, F. Mancini, S. Odashima, *Physica C* **388**, 76 (2003)
27. A. Avella, F. Mancini, S. Odashima (2003), preprint of the University of Salerno, to be published in *J. Magn. Magn. Mater.*